

First principle study of the magnetism of $\text{Sr}_2\text{CoMoO}_{6-\delta}$ ($\delta = 0, 1/2$) double perovskites

C. Etz^a and D. Stoeffler^b

Institut de Physique et de Chimie des Matériaux de Strasbourg (UMR 7504 CNRS -ULP), 23 rue du Loess, BP 43, 67034 Strasbourg Cedex 2, France

Received 23 June 2006 / Received in final form 18 December 2006

Published online 17 January 2007 – © EDP Sciences, Società Italiana di Fisica, Springer-Verlag 2007

Abstract. We investigate the electronic structure of bulk $\text{Sr}_2\text{CoMoO}_{6-\delta}$ double perovskites using the ab initio Full Potential Linearized Augmented Plane Wave method in order to study their magnetic properties within the GGA and GGA+U methods. We discuss the relative stability of ferromagnetic (FM) and antiferromagnetic (AFM) orders (i) without and with taking into account the observed tilting of the oxygen octahedra and (ii) by introducing oxygen vacancies. We show that a very good agreement with experimental results — AFM order for $\delta = 0$ and FM order for $\delta = 1/2$ — is obtained only when the tilting of the oxygen tetrahedra is taking into account and when the GGA+U method is used.

PACS. 71.20.-b Electron density of states and band structure of crystalline – 71.55.Ak Metals, semimetals, and alloys – 75.47.-m Magnetotransport phenomena; materials for magnetotransport

1 Introduction

The potential use of magnetic oxide as electrode into spintronic devices has stimulated theoretical investigations, in terms of magnetic ordering and spin dependent band structure (BS), aiming to predict their capability to spin polarize a current [1, 2]. $\text{Sr}_2\text{FeMoO}_6$ (SFMO) double perovskite (DP) is a candidate for such materials due to (i) its predicted half-metallic (HM) character (it acts as an insulator for one spin channel and like a metal for the other one) and (ii) its ferromagnetic ordering up to 415 K. However, the preparation of these oxides being hard to achieve without structural and chemical imperfections, the expected properties have not yet been clearly exhibited. If usual Density Functional Theory (DFT) using Local Density (LDA) or Generalized Gradient (GGA) Approximation allows a correct description the electronic structure of DP, it usually fails to predict the correct most stable magnetic solution when antisite [3] or antiferromagnetic order are considered. Previous works [4, 5] have shown the importance of the Hubbard contribution (within the GGA+U method) by combining electronic structure calculations and photoemission spectroscopy results. However, its role on the stability of magnetic orders in DP has not been considered. Using GGA+U has also a significant impact on the electronic structure by enhancing the insulating character of the bands and cannot be ne-

glected when it is aimed to use these DP materials for spin transport devices.

Recently, $\text{Sr}_2\text{CoMoO}_6$ (SCMO) DP, the Co analogous to SFMO, have been synthesized using a “chimie douce” method and have been characterized by neutron powder diffraction [6]. At room temperature, the crystal structure is found tetragonal (space group $I4/m$) with $a = 5.565 \text{ \AA}$ and $c = 7.948 \text{ \AA}$ and contains alternating CoO_6 and MoO_6 octahedra tilted by 7° in the basal ab plane (Fig. 1). The stoichiometric samples are found antiferromagnetic ($T_N = 37 \text{ K}$) and insulating. The reduction of these samples, leading to oxygen-deficient perovskites with the same crystal structure, gives rise to ferromagnetic domains ($T_C = 350$ to 370 K) and to a dramatic increase of the conductivity related to a large component of itinerancy for down-spin $\text{Mo } t_{2g}$ electrons.

In this paper, we investigate the electronic structure of SCMO and we simulate the occurrence of O vacancies (O^*) taking electronic correlation into account in the DFT within the GGA+U approach (GGA including the semi-empirical Hubbard contribution). We show that it changes significantly the results of the DFT calculations and gives a good agreement with experiment.

2 Method

We calculate self-consistently the BS for the considered DP systems in the full potential augmented plane wave formalism (FLAPW) in the FLEUR implementation [7] using the GGA without and with the Hubbard contribution (GGA+U) and taking core, semi-core and valence

^a Present address: Center for Computational Materials Science (CMS) Gumpendorferstrasse 1A A-1060 Vienna, Austria.

^b e-mail: Daniel.Stoeffler@ipcms.u-strasbg.fr

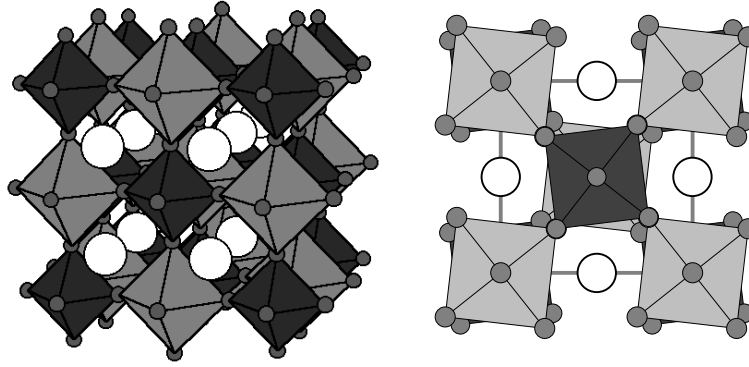


Fig. 1. Schematic representations of the $\text{Sr}_2\text{CoMoO}_6$ unit cell displaying tilted octahedra: (left) 3D view of the cell containing 4 formula units and (right) top view of the cell containing 2 formula units. The white (respectively gray) spheres correspond to Sr (respectively O) atoms and the light (respectively Dark) gray octahedra are centered on Co (respectively Mo) atoms.

Table 1. Internal atomic position for all inequivalent sites for the 2 structures considered.

$(I4/mmm) / (I4/m)$	site	x	y	z
Sr	$4d$	0/0	0.5/0.5	0.25/0.25
Co	$2a$	0/0	0/0	0/0
Mo	$2b$	0/0	0/0	0.5/0.5
O1	$4e$	0/0	0/0	0.2500/0.2589
O2	$8h$	0.2500/0.2895	0.2500/0.2296	0/0

states into account. All calculations are carried out for a set of increasing \mathbf{k} -points until no variation into the main results is reached. More precisely, for the cases without O vacancies, we used up to 84 ($I4/mmm$ symmetry) or 75 ($I4/m$ symmetry) special \mathbf{k} -points in the irreducible wedge of the Brillouin zone and for the case with O vacancies, we used up to 48 special \mathbf{k} -points during the self-consistent calculations. An energy convergence of 10^{-5} Hartree is reached and, for successive sets with increasing numbers of \mathbf{k} -points, the variation of the total energy was smaller than 2×10^{-4} Hartree. Finally, each density of states is calculated using 385 ($I4/mmm$ symmetry), 384 ($I4/m$ symmetry) and 540 (O vacancies) \mathbf{k} -points and is slightly smeared only outside band gaps.

In order to examine the stability of the experimental structure, we should relax the cell parameters (a , c) and the internal degree of freedom like the z_1 position of the oxygen atom (O1) linking Co and Mo into the c direction and the position (x_2 , y_2) of the O atom (O2) in the basal plane (see Tab. 1). However, such a calculation requires too much computer time. Nevertheless, aiming to investigate the role of the tilted octahedra, we have done a partial relaxation varying only a and c into the $I4/mmm$ symmetry (where $z_1 = x_2 = y_2 = 1/4$). The comparison between this relaxed $I4/mmm$ structure and the experimental one will give us strong indications about the role of the tilting (mainly because the experimental structure will finally be the most stable one).

3 $I4/mmm$ relaxed structure

We have determined the values of a and c minimizing the total energy by interpolating the values calculated for a set

of (a , c) points on a grid. The energy minimum is obtained for $a = 5.61$ Å and $c = 7.93$ Å. It is not surprising to find a slightly larger ab basal plane parameter than the experimental value because the octahedra tilting affects more especially in-plane Co-O-Mo bonds and leads to a reduction of the Co-Mo distance.

The densities of states (DOS) for the ferromagnetic (FM) solution within GGA, displayed in Figure 2, are very similar to the ones obtained for SFMO [3]: the spin-up DOS exhibits a gap (ranging from -0.1 to 0.7 eV) around the Fermi level (E_F) separating mainly Co occupied states from mainly Mo t_{2g} unoccupied states whereas the down-spin DOS shows a metallic behaviour. As a consequence of this half-metallic character, the total moment is equal to $3 \mu_B$ per formula unit (f.u.). For the antiferromagnetic (AFM) solution, built by considering a unit cell containing 2 f.u. with opposite magnetic moments on the 2 Co sites (the up- and down-spin DOS are identical), we found finite DOS at E_F indicating metallic behaviour. However, the FM solution is found to be the most stable by 117 meV per 2 f.u. cell. Consequently, the SCMO is found half-metallic and ferromagnetically ordered for this $I4/mmm$ structure with the GGA method.

As we will see later, the energy difference between antiferromagnetic (AFM) and ferromagnetic (FM) solutions ($\Delta E_{AFM-FM} = E_{AFM} - E_{FM}$) is found small (a few meV/cell) when the GGA+U method is used; that can make the choice of the U and J parameters of the Hubbard Hamiltonian very questionable. In the literature, usual values for Co are $U_{Co} = 5$ eV and $J_{Co} = 0.89$ eV which makes U_{Co} particularly large as compared to the resulting total energy difference. In order to investigate the role of these 2 parameters, we have varied U and J over a reasonable range of values (see Tab. 2) and found very

Table 2. Energy difference between ferromagnetic (FM) and antiferromagnetic (AFM) solutions in meV per cell (a cell corresponds to 2 f.u.) for the 2 structures considered for various U and J values of the GGA+U method (for comparison, with the GGA method we get $\Delta E_{AFM-FM} = 117 / 142$ meV/cell).

ΔE_{AFM-FM} (meV/cell) ($I4/mmm$)/($I4/m$)	$J = 0.78$ eV	$J = 0.89$ eV	$J = 1.00$ eV
$U = 3$ eV	-34/-14	-32/-13	-32/-18
$U = 4$ eV	-28/-10	-26/-8	-21/-3
$U = 5$ eV	-22/-8	-20/-7	-18/-6

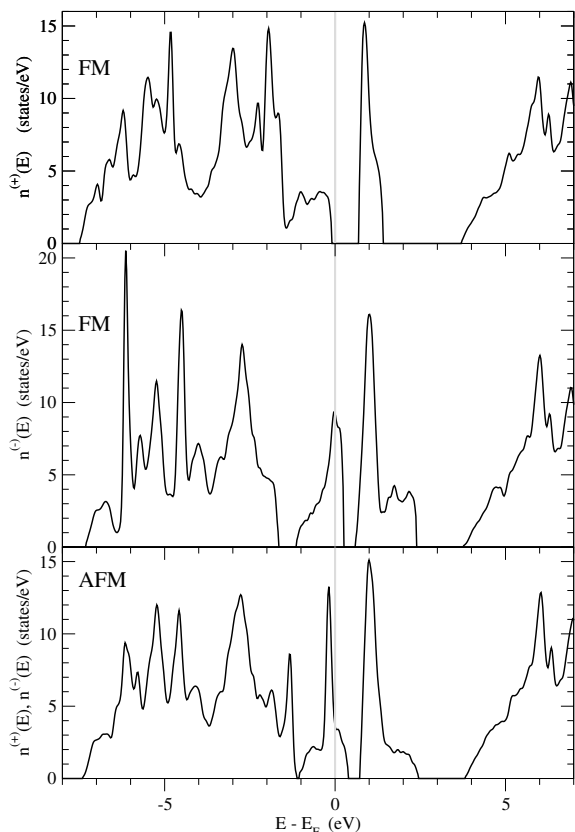


Fig. 2. Densities of states (DOS) for $\text{Sr}_2\text{CoMoO}_6$ in the $I4/mmm$ unit cell obtained by minimization of the total energy for ferromagnetic (FM) and antiferromagnetic (AFM) solutions using the GGA method. The vertical gray line corresponds to the Fermi level (E_F), $n^{(+)}$ ($n^{(-)}$) corresponds the up-spin (respectively down-spin) DOS.

smooth variations of ΔE_{AFM-FM} (its absolute value increases even when U and J are reduced) without change of sign. This is a clear indication of the reliability of these calculations and we will use $U_{\text{Co}} = 5$ eV and $J_{\text{Co}} = 0.89$ eV for all other GGA+U calculations in this work [8].

With the GGA+U method and for the FM solution, giving also a total moment of $3 \mu_B/\text{f.u.}$, both spin DOS (Fig. 3) present a gap around E_F : the gap into the down-spin DOS coming from the splitting of the Fe and Mo states (the Fe states are shifted towards lower energy whereas the Mo ones are shifted towards higher energy). This illustrates the major contribution of the GGA+U

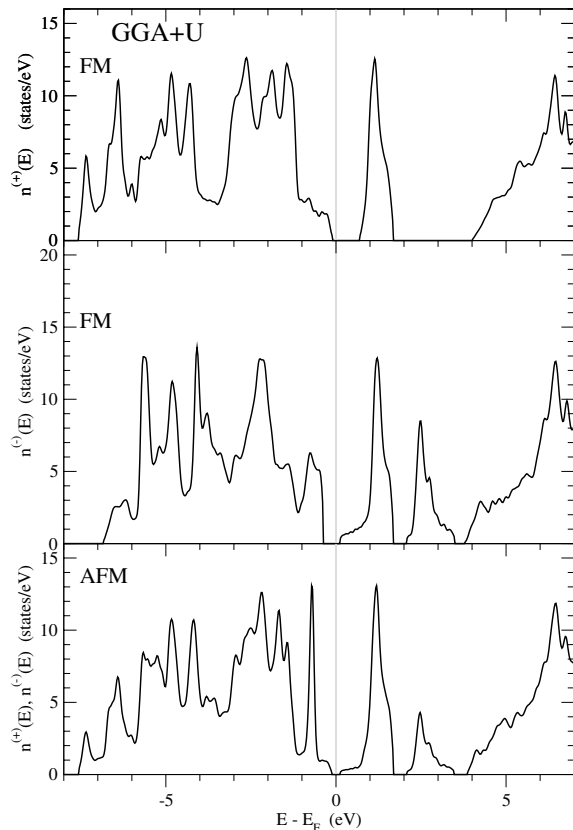


Fig. 3. Densities of states (DOS) for $\text{Sr}_2\text{CoMoO}_6$ in the $I4/mmm$ unit cell obtained by minimization of the total energy for ferromagnetic (FM) and antiferromagnetic (AFM) solutions using the GGA+U method. The vertical gray line corresponds to the Fermi level (E_F), $n^{(+)}$ ($n^{(-)}$) corresponds the up-spin (respectively down-spin) DOS.

method: it shifts occupied states to lower energy and unoccupied states to higher energy resulting usually in the occurrence of new gaps or the enlargement of gaps around E_F . A similar result is obtained for the AFM solution presenting a small gap (from -0.11 to 0.11 eV). However, contrary to the results of the GGA method, the AFM solution is found to be more stable by 20 meV/cell than the FM one. Consequently, the SCMO is found insulating and antiferromagnetically ordered for the $I4/mmm$ structure with the GGA+U method, this result being clearly more satisfactory when compared to the experiments.

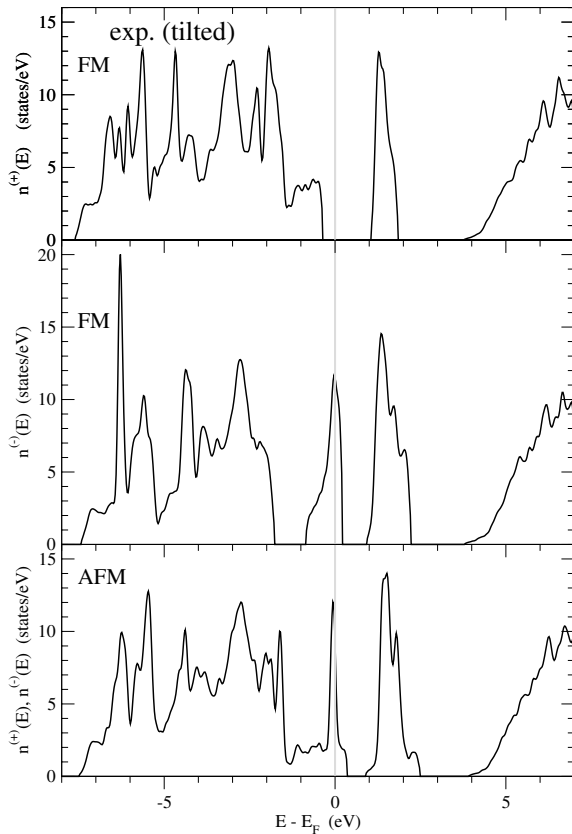


Fig. 4. Densities of states (DOS) for $\text{Sr}_2\text{CoMoO}_6$ in the $I4/m$ unit cell with tilted octahedra for ferromagnetic (FM) and antiferromagnetic (AFM) solutions using the GGA method. The vertical gray line corresponds to the Fermi level (E_F), $n^{(+)}$ ($n^{(-)}$) corresponds the up-spin (respectively down-spin) DOS.

4 Experimental $I4/m$ structure

This structure introduces only limited modifications relative to the previously considered $I4/mmm$ one: the neighbourhood of each Co or Mo atom remains the same in terms of O coordination and only the volume of the octahedra is slightly altered (the O-Co and O-Mo distances vary by $\pm 3.6\%$ in the ab plane). Consequently, we do not expect the main structures in the DOS to be affected. However, because the 4 in plane ab Co-O-Mo bonds are no more rectilinear, the interaction between Co and Mo states can be significantly changed affecting directly the gap between occupied Co and unoccupied Mo states. This is exactly what we obtain.

With the GGA method (Fig. 4), the DOS are very similar to the previous ones (Fig. 2) and exhibit more narrow structures separated by larger gaps (for example, the gap around E_F in the spin-up DOS for the FM solution ranges from -0.35 to 1.05 eV and is nearly doubled) indicating clearly more tight Co-O-Mo bonds. The AFM solution is found to be also less stable than the FM one by 142 meV/cell. Surprisingly, this FM solution is 457 meV/cell less stable into the $I4/m$ crystal structure than the corresponding FM solution into the $I4/mmm$ crystal structure. This difference can be hardly overcome

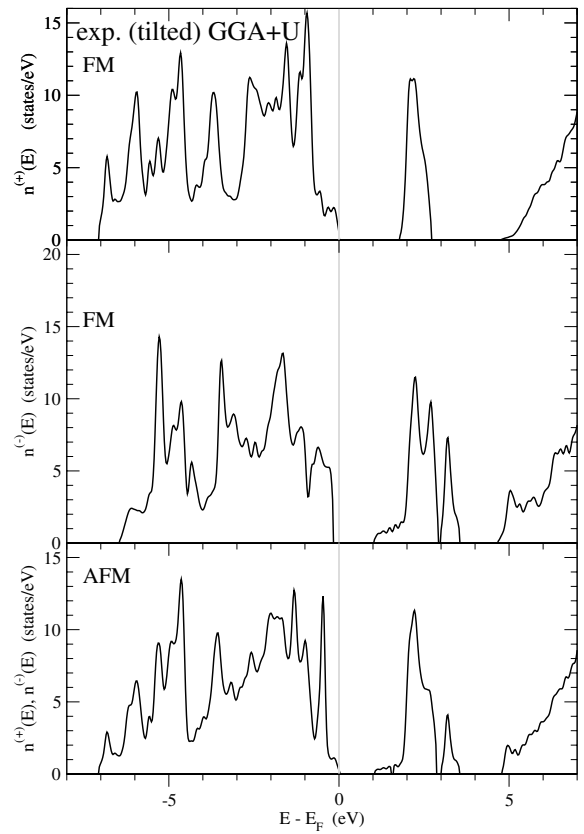


Fig. 5. Densities of states (DOS) for $\text{Sr}_2\text{CoMoO}_6$ in the $I4/m$ unit cell with tilted octahedra for ferromagnetic (FM) and antiferromagnetic (AFM) solutions using the GGA+U method. The vertical gray line corresponds to the Fermi level (E_F), $n^{(+)}$ ($n^{(-)}$) corresponds the up-spin (respectively down-spin) DOS.

by internal relaxations. Consequently, the disagreement with the experimental results becomes more pronounced with the GGA method: the $I4/mmm$ crystal structure is the most stable and ferromagnetism is favoured to antiferromagnetism.

With the GGA+U method (Fig. 5), an insulating behaviour is obtained for both FM and AFM solutions with enlarged gaps as compared to the ones of Figure 2 and the AFM solution is also the most stable one by 7 meV/cell. The major new result of this calculation is that, for the AFM solution, the $I4/m$ crystal structure is 160 meV/cell more stable than the $I4/mmm$ one (for the FM solution). Even if this result does not prove that the present $I4/m$ structure is the most stable one, this shows clearly that internal relaxations have to be taken into account. Consequently, we found a complete agreement with the experiment with the GGA+U method: the experimental $I4/m$ crystal structure is more stable than all other $I4/mmm$ ones and the SCMO is an antiferromagnetic insulator. In the following, we consider only the case of GGA+U calculations for the discussion.

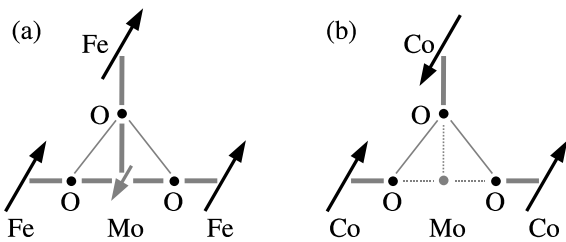


Fig. 6. Sketch of the bonds into (a) $\text{Sr}_2\text{FeMoO}_6$ and (b) $\text{Sr}_2\text{CoMoO}_6$. The strength of the interatomic interaction is given by the style of the line representing the bond where the strongest is the thick solid line, the weakest is the thin dashed line and the medium is the thin solid line.

5 Comparison with a Super-Exchange Based Model (SEBM)

Usually, to explain the magnetic and the electronic properties of SFMO DP, a model based on a super-exchange coupling of two successive large and positive Fe moments to a common small and negative Mo moments is used: Fe^{3+} ($3d^5$) ions carrying a $5 \mu_B$ magnetic moment are negatively coupled to Mo^{5+} ($4d^1$) ions carrying a $1 \mu_B$ magnetic moment via a ferrimagnetic super-exchange mechanism involving the O atom in between the Fe and Mo atoms. This model explains well the ferromagnetic order obtained on the Fe sublattice by considering Fe-O-Mo-O-Fe chains where two successive Fe moments are negatively coupled to a common Mo moment (Fig. 6a). It explains also the HM property giving (i) a completely filled Fe $3d$ (t_{2g} and e_g) up-spin band fully splitted (by a gap resulting from the super-exchange) from the empty Mo $4d$ (t_{2g}) up-spin band and (ii) a partially filled Mo $4d$ (t_{2g}) down-spin band. Consequently, the major feature at the origin of the ferromagnetic half-metallic state is the single conduction electron into the down spin $4d$ shell of Mo. Explicit BS calculations, using the GGA+U method, agree with the main conclusions of the SEBM (Ferromagnetic half-metal with a total magnetic moment of $4 \mu_B/\text{f.u.}$) but not with the considered local moments: Fe and Mo carry respectively a moment of $4 \mu_B$ and $-0.4 \mu_B$.

Considering SCMO, an insulating AFM solution is found to be the most stable within our calculations. This agrees with the SEBM only if we assume than we have Co^{2+} ($3d^7$) ions carrying a $3 \mu_B$ magnetic moment and Mo^{6+} ($4d^0$) ions carrying no magnetic moment. With such a configuration, no d electrons are available on the Mo site giving the insulating behaviour and no super-exchange interaction can take place for coupling the Co magnetic moments with a common Mo one. Indeed, only an antiferromagnetic super-exchange mechanism can occur involving two Co moments coupled through two directly linked O atoms comprised in the octahedra surrounding the Mo atom which is situated at the corner of the Co-Mo-Co 90° bond (Fig. 6b). Instead of having the magnetic coupling dominated by Co-O-Mo-O-Co chains, like in SFMO, the coupling is dominated by Co-O-O-Co ones. Consequently, the two Co moments are negatively coupled giving rise

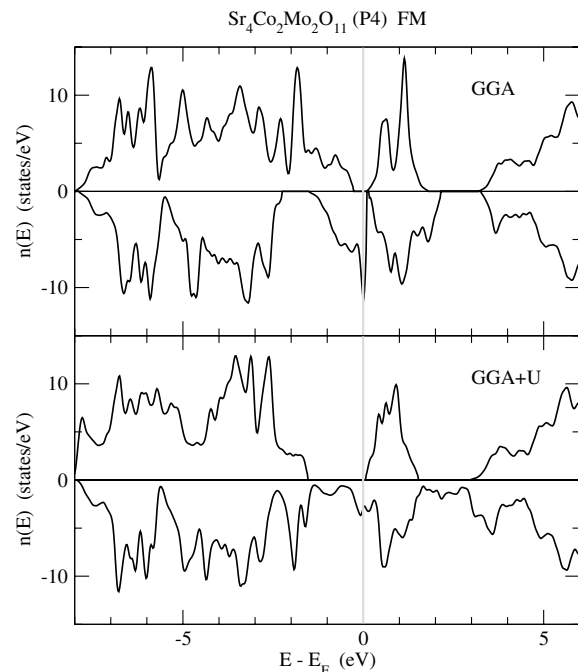


Fig. 7. Densities of states (DOS) for $\text{Sr}_4\text{Co}_2\text{Mo}_2\text{O}_{11}$ in the $I4/m$ unit cell with tilted octahedra for ferromagnetic solutions using the GGA and the GGA+U methods. The vertical gray line corresponds to the Fermi level (E_F), the down-spin DOS is displayed with negative values.

to an antiferromagnetic order. Like for SFMO, this model does not agree with our explicit BS calculations (using the GGA+U method) when considering local moments and charge occupation: Co and Mo atoms carry respectively a moment of $\pm 2.7 \mu_B$ and $\pm 0.02 \mu_B$ and the $4d$ states of Mo show a significant occupation. However, a close look to the DOS shows that these occupied Mo states are very deep in energy (around -5 eV below the Fermi level) and there are effectively no Mo states available above -2 eV even if the configuration is not strictly $4d^0$.

We conclude that BS calculations and the SEBM lead to the same conclusion when the charge occupations obtained from the BS calculations allow the SEBM to be applied.

6 Oxygen deficient case

Experimentally, it has been shown that ferromagnetism is recovered and that the resistivity is decreased for the oxygen-deficient samples. Using the SEBM as a guide, this can be understood by considering that the removal of oxygen atoms adds two electrons to the delocalized charge per O vacancy and that a fraction of this additional electronic charge is gained by the Mo atoms in the vicinity of the vacancy. Consequently, $4d$ electrons become available on these Mo sites carrying a negative local magnetic moment and resulting in a ferromagnetic coupling between Co moments mediated by the Mo one like in SFMO.

Experimentally, it has been shown that the structure of oxygen-deficient samples is very similar to the

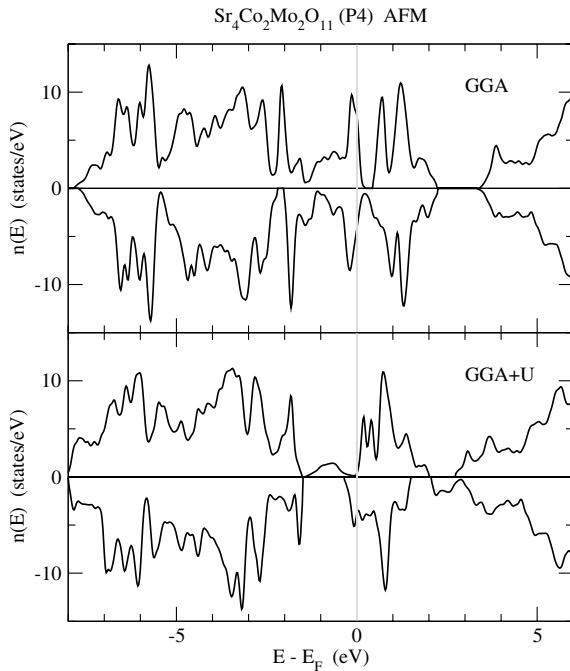


Fig. 8. Densities of states (DOS) for $\text{Sr}_4\text{Co}_2\text{Mo}_2\text{O}_{11}$ in the $I4/m$ unit cell with tilted octahedra for antiferromagnetic (AFM) solutions using the GGA and the GGA+U methods. The vertical gray line corresponds to the Fermi level (E_F), the down-spin DOS is displayed with negative values.

stoichiometric ones [6]. Consequently, we assume that an oxygen vacancy induces no structural relaxations and our cell is built starting from the same $I4/m$ cell and removing one O atom of a Co-O-Mo link along the c direction corresponding to a lower symmetry space group. We have done the calculation for $\text{Sr}_4\text{Co}_2\text{Mo}_2\text{O}_{11}$, corresponding to a much higher O vacancy concentration than the experimental one, and we get the FM solution to be more stable than the AFM one with both GGA ($\Delta E_{FM-AFM} = -95$ meV/cell) and GGA+U ($\Delta E_{FM-AFM} = -76$ meV/cell) methods. As expected, we recover clearly Mo states around the Fermi level and the magnetic moment on the Mo site having an O^* as neighbour is found large ($-0.45 \mu_B$ for FM and $-0.26 \mu_B$ for AFM). Finally, the DOS (Figs. 7 and 8) show clearly that the stabilization of a FM solution corresponds to a half-metallic electronic structure in perfect agreement with the observed increase of the conductivity for this situation.

7 Conclusion and outlook

To summarize, we have shown that the use of the GGA+U method allows us to get a perfect agreement between the calculated and observed magnetic and electronic properties: (i) SCMO is an antiferromagnetic insulator for the most stable $I4/m$ crystal structure presenting tilted oxygen octahedra and (ii) it becomes half-metallic and ferromagnetic when oxygen vacancies are present. We have analyzed our results by comparison with a super-exchange base model and we have shown that both approaches lead to the same conclusions but the model has to be used carefully and gives only trends.

The fair agreement between calculated and measured magnetic and transport properties confirms that the present approach has the ability to describe accurately such kind of systems. Future works will focus on the reduction of the oxygen vacancies concentration by increasing the cell and on the role played by Co or Mo antisites.

The authors thank S. Colis and A. Dinia for stimulating discussions and the Centre d'Études du Calcul Parallèle et de la Visualisation (<http://www-cecpv.u-strasbg.fr>) of University Louis Pasteur for computing facilities. C. Etz acknowledges the financial support from the ERASMUS program and the hospitality of the IPCMS.

References

1. K.I. Kobayashi, T. Kimura, H. Sawada, K. Terakura, Y. Tokura, *Nature* **395**, 677 (1998)
2. D.D. Sarma, *Phys. Rev. Lett.* **85**, 2549 (2000)
3. D. Stoeffler, S. Colis, *J. Phys.: Condens. Matter.* **17**, 6415 (2005)
4. T. Saitoh et al., *Phys. Rev. B* **66**, 035112 (2002)
5. Sugata Ray et al., *Phys. Rev. B* **67**, 085109 (2003)
6. M.C. Viola et al., *Chem. Mater.* **14**, 812 (2002)
7. FLEUR is an implementation of the Full Potential Linearized Augmented Plane Wave method freely available at <http://www.flapw.de> funded by the European Research Network Ψ_k and managed by Prof. S. Blugel
8. As a test, we have also done a calculation with $U_{\text{Mo}} = 3$ eV but, compared to the results obtained with $U_{\text{Mo}} = 0$ eV, the densities of states and the energy difference between FM and AFM solutions were nearly not affected